SCIENCE CHINA
Physics, Mechanics & Astronomy

• **Article** •

November 2016 Vol. 59 No. 11: 114711
doi: 10.1007/s11433-016-0288-8

Analytic prediction for planar turbulent boundary layers†

Xi Chen, and Zhen-Su She*

State Key Laboratory for Turbulence and Complex Systems and Department of Mechanics, College of Engineering, Peking University, Beijing 100871, China

Received July 20, 2016; accepted August 18, 2016; published online September 19, 2016

Analytic predictions of mean velocity profile (MVP) and streamwise (x) development of related integral quantities are presented for flows in channel and turbulent boundary layer (TBL), based on a symmetry analysis of eddy length and total stress. Specific predictions include the relations for momentum Reynolds number (Re_θ) with friction Re_τ and streamwise Re_x: $Re_\theta \approx 3.27Re_\tau$, and $Re_x/Re_\theta = 4.94[(\ln Re_\theta + 1.88)^2 + 1]$; the streamwise development of the friction velocity u_τ: $U_e/u_\tau \approx 2.22\ln Re_x + 2.86 - 3.83\ln(\ln Re_x)$, and of the boundary layer thickness δ_e: $x/\delta_e \approx 7.27\ln Re_x - 5.18 - 12.52\ln(\ln Re_x)$, which are fully validated by recent reliable data.

turbulent boundary layer, symmetry analysis, eddy length, log law

PACS number(s): 47.27.-i, 47.27.N-, 47.27.E-

Citation: X. Chen, Z. S. She, Analytic prediction for planar turbulent boundary layers, Sci. China-Phys. Mech. Astron. **59**, 114711 (2016), doi: 10.1007/s11433-016-0288-8

1 Introduction

Planar turbulent boundary layer (channel and TBL) is a canonical wall-bounded flow of significant theoretical and practical interests [1]. It is widely seen in the atmospheric flows near the ground, or the flows over the surface of a vessel, or the wings of an aircraft, etc. [2], and has attracted constant efforts [3-7]. Common to all these flows is a thin-layer close to the wall - named turbulent boundary layer [8] - where most of flow momentums and energies are dissipated by viscous drag and turbulent fluctuations. The latter two effects have been studied since Reynolds [9], with the usage of the ensemble averaged Navier-Stokes equation

$$\nu\partial_y U - \langle u'v'\rangle = \tau, \tag{1}$$

where U is the streamwise mean velocity, u' and v' are streamwise and normal fluctuating velocity, respectively, ν the molecular viscosity and τ the total stress representing the driving force (defined later). This equation is unclosed in the presence of fluctuating velocities, and the long-standing question is how to predict U for all Reynolds numbers, and then the streamwise development of other relevant quantities (including the friction coefficient) [1]. Until today, it is still a vivid challenge to theorists [10], despite over a century's effort since the seminar work of Prandtl in 1904 proposing the concept of the boundary layer [8].

In modern analysis, the difficulty of the problem is particularly attributed to the interplay of two different characteristic scales [11]. Denote $S = \partial_y U$, the mean shear, $W = -\langle u'v'\rangle$ the turbulent Reynolds shear stress. When the leading balance of eq. (1) is between νS and τ, which occurs in the inner flow region close to the wall, the friction velocity (u_τ) and viscous length ($\ell_\nu = \nu/u_\tau$) define the correct scales exhibiting data collapse of U at different Re's, known as the law of wall. However, for outer flow ($\ell_\nu \ll y \leqslant \delta_e$, δ_e the boundary layer thickness commonly set as δ_{99}) where $\nu S \ll W$, choosing u_τ or U_e (freestream velocity) as the velocity scale would respectively lead to log law [12] or power law [13, 14] description of U in an intermediate overlap region for asymp-

*Corresponding author (email: she@pku.edu.cn)

†Contributed by Zhen-Su She (Associate Editor)

totically large Re's. The debate between the two proposals continues to attract attention [10], for both allow a satisfactory description of data in their restricted flow regions. On the other hand, more empirical approaches [15, 16] introduce composite formulas describing the mean velocity for the entire domain, but with many free parameters of pure fitting. In short, analytic approach with clear physical picture and testable assumptions is missing, leaving important questions as the universality of Karman constant, and effects of geometry (internal versus external flows) unaddressed.

Here, we propose a symmetry-based approach yielding a closure solution for the mean momentum and kinetic energy equations. Our analysis begins with a symmetry analysis of a characteristic length of energy containing eddy, which enables a prediction of its functional form. It also quantifies the geometry difference between channel and TBL, through different approximations of kinetic energy equation as well as the total stress, thus going beyond a recent theory of channel by L'vov et al. [17] (here referred to as LPR). The predicted mean velocity covers the entire outer flow domain; and in the case of TBL, the streamwise developments of a series of global quantities, i.e. friction coefficient, shape factor, boundary layer and momentum thicknesses, are predicted, agreeing well with data. Compared to previous Pades approximations [16] (here referred to as MCN) and multilayer models [15], the current theory involves only three parameters for TBL (and for channel), which are Re-independent; in particular, the Karman constant $\kappa \approx 0.45$ is remarkably universal in channel and TBL (also applied to pipes [18]). The result resolves the "log-law and power-law" debate on the scaling of mean velocity, in favor of the log law, but with corrections beyond the leading order in $1/\ln Re_\tau$.

2 Theory

For the flow over a flat plate ($0 \leqslant x \leqslant \infty$ and $y = 0$), the Navier-Stokes-Prandtl equations read

$$\partial_x U + \partial_y V = 0, \tag{2}$$

$$U\partial_x U + V\partial_y U + \partial_x P = \nu\partial_y\partial_y U - \partial_y \langle u'v'\rangle, \tag{3}$$

where V the mean vertical velocity (zero in channel) and $\partial_x P$ the mean pressure gradient (zero in TBL). Integrating eq. (3) in y yields eq. (1), where for channel $\tau = u_\tau^2 r'$ ($r' = r/\delta_e$ and $r = \delta_e - y$; δ_e the half height of a channel), and for TBL $\tau = u_\tau^2 + \int_0^y (U\partial_x U + V\partial_{y'} U)\mathrm{d}y'$. Substituting eq. (2) into eq. (3) and integrating the latter from 0 to δ_e, one obtains the von Karman's integral momentum equation for TBL

$$\mathrm{d}\theta/\mathrm{d}x = u_\tau^2/U_e^2 = C_f/2, \tag{4}$$

where $\theta = \int_0^{\delta_e} U/U_e(1 - U/U_e)\mathrm{d}y$ is the momentum thickness, and $C_f = 2u_\tau^2/U_e^2$ is the friction coefficient (here we set zero S and W for $y \geqslant \delta_e$). Moreover, the turbulent kinetic energy is described by the mean kinetic energy equation, i.e.

$$SW + \Pi = \varepsilon, \tag{5}$$

where $\mathcal{P} = SW$ is the production; Π represents the spatial energy transfer (including diffusion, convection and fluctuation transport); ε is the viscous dissipation. Note that eqs. (1) and (5) describe the two fundamental processes in the flow, i.e. momentum and energy transports, respectively; and eq. (4) characterizes the streamwise scaling of friction coefficient for TBL. We now construct a closure solution as below.

Note that according to eq. (5), ε should be determined by S and W, and a characteristic length ℓ describing the effects of spatial energy transfer Π. Thus, a dimensional argument yields $\varepsilon(S, W, \ell) = W^{(1+\frac{n}{2})}S^{(1-n)}\ell^{(-n)}$ or

$$\ell = W^{(\frac{1}{n}+\frac{1}{2})}S^{(\frac{1}{n}-1)}\varepsilon^{(-\frac{1}{n})}, \tag{6}$$

where n is an arbitrary real number. Note that as $n \to \infty$, the dissipation drops out, and the resulting length becomes the classical mixing length of Prandtl [8]: $\ell_\infty = \sqrt{W}/S$. Furthermore, for a channel flow, $S \propto r$ due to the central mirror symmetry, and eq. (1) can be approximated to $W \approx \tau \propto r$. Meanwhile, ε tends to $\varepsilon_0 > 0$ as $r \to 0$. Thus, eq. (6) yields $\ell \propto r^{\frac{2}{n}-\frac{1}{2}}$, where only $n = 4$ results in a finite nonzero value ℓ_0 at $r = 0$. Hence a unique characteristic length ℓ_ε is defined as:

$$\ell_\varepsilon = W^{\frac{3}{4}}S^{\frac{-3}{4}}\varepsilon^{\frac{-1}{4}} = \nu_T^{3/4}\varepsilon^{\frac{-1}{4}}, \tag{7}$$

where $\nu_T = W/S$ is the eddy viscosity. Note that, the ratio between ℓ_ε and any other length of different n's in eq. (6) is exactly related to the dissipation production ratio, $\Theta \equiv \varepsilon/(SW)$, namely $\ell_n/\ell_\varepsilon = \Theta^{\frac{1}{4}-\frac{1}{n}}$, Interestingly, when $\Theta \approx 1$ corresponding to the well-known quasi-balance regime (QBR), all lengths reduce to a single one, namely ℓ_ε.

Near the centerline of a channel (where we call the core layer), $\Theta \propto r^{-2}$, and all lengths are different. A simple matching argument can derive an expression for Θ, valid from QBR to central core. Assume $\Theta \approx c/r'^2$ as $r' \to 0$, where c is a dimensionless coefficient. To match $\Theta \to 1$ as $r' \to 1$, a composite expression is $\Theta = 1 + c/r'^2 - c$, which can be rewritten as:

$$\Theta(r') = [1 + (r_\mathrm{c}/r')^2]/(1 + r_\mathrm{c}^2), \tag{8}$$

where $r_\mathrm{c} = \sqrt{c/(1-c)}$ indicates the thickness of the core layer (given later). A variant of eq. (8) is for the spatial energy transfer in eq. (5), that is $\Pi = \mathcal{P}(\Theta - 1) \propto (1 - r'^2)$. The parabolic form stems from the simplest expansion at $r = 0$ in the presence of the central mirror symmetry, namely, $\partial_r\Pi = 0$. Hence, eq. (8) is a reasonable approximation, which solves eq. (5).

Interestingly, ℓ_ε can be contrasted to the Kolmogorov dissipation length $\eta = \nu^{3/4}/\varepsilon^{1/4}$. In the classical Kolmogorov argument about η, ε is the rate of energy cascade in the inertial range, while ν is the molecular viscosity, transferring the kinetic energy to heat. So, Kolmogorov's η can be interpreted as a length where the balance between the inertial energy cascade and molecular dissipation takes place. We thus interpret ℓ_ε also as a length of the balance between ε and ν_T. But here, the role of ν_T is reversed: instead of dissipating energy (out) to heat, it really pulls the energy in since S and W (and its product) generate turbulent fluctuations (and so-called production). In other words, ℓ_ε is interpreted to be the integral eddy size where the eddy "viscosity" produces the kinetic energy through the mean shear, and where this energy is transferred out to smaller scales through the energy cascade. Note that this length recovers the crucial scaling function in the LPR model [17] without involving any wall function.

For TBL, $\ell_\varepsilon = \nu_T^{3/4}\varepsilon^{-\frac{1}{4}}$ can be defined in the same way. It is important to emphasize that this extension is highly non-trivial, since it has never been realized that there exists a critical point near the edge of the boundary layer, which plays a similar role as the centerline of a channel (i.e. $r = 0$). For TBL, this is the point where the QBR ends and where ℓ_ε takes a maximum, suggesting the integral eddy grows to the maximum size. The existence of this point brings in a crucial new physics which simplifies the matter and yields an analytic expression presented below. Note that eq. (8) also applies to TBL, where $r' = \delta_e - y$ the distance to the boundary layer edge, and $r_c = 0$ (hence $\Theta \equiv 1$).

Now, we develop a symmetry argument to derive the functional form of ℓ_ε and τ. It consists in postulating a scaling form originated from a dilation invariance in the direction normal to the wall. The key element is the dilation center, or the fixed point for dilation transformation group, which is located at $r = 0$ for ℓ_ε where $\ell_\varepsilon = \ell_\varepsilon^{\max} = \ell_0$, and at $y = 0$ for τ where $\tau = \tau^{\max} = \tau_w$. In both cases, we assume that the dilation invariant form is $\mathrm{d}\ell_\varepsilon/\mathrm{d}r \propto r^\alpha$ and $\mathrm{d}\tau/\mathrm{d}y \propto y^\beta$, since $\mathrm{d}\ell_\varepsilon/\mathrm{d}r = 0$ at $r' = 0$ and $\mathrm{d}\tau/\mathrm{d}y = 0$ at $y = 0$.

For ℓ_ε, the boundary condition at the wall, i.e. $\ell_\varepsilon = 0$ at $r' = 1$, yields a defect power law form: $\ell_\varepsilon/\ell_0 = 1 - r'^m$, with $m = \alpha + 1$ a free parameter characterizing the scaling for the bulk flow. This dilation center at $r = 0$ may seem to be natural for channel, but highly non-trivial for TBL, for which the boundary layer edge (δ_e) has never been realized to play a similar role before. Note that this assumption was validated by DNS data with $m = 4$ for planar turbulent boundary layers [19, 20], enabling a simple analytic theory for TBL since Prandtl [8]. A further argument supporting the similarity is that ℓ_ε reaches the maximum in both channel and TBL, signifying that the eddies are self-organized in both flows in the same manner around this center ($r = 0$). In order words, the defect power law of ℓ_ε characterizes the similarity form of the same ensemble of eddies in both outer flows (i.e. channel and TBL), which are probably the detached eddies as postulated by Perry [21]. Further study will confirm whether they have the same statistics, just like the wall-attached eddies showing self-similarity in the near-wall region [22].

Note also that the defect law has a right asymptotic close to the wall ($r' \to 1$): $1 - r'^4 \approx 4y/\delta_e$ and $\ell_\varepsilon \approx 4y(\ell_0/\delta_e)$, which is consistent with the recent studies that the scale of large eddies is proportional to the wall distance [22]. Denoting $4\ell_0/\delta_e = \kappa$ (so that $\ell_\varepsilon \approx \kappa y$ when $r' \to 1$), the form of ℓ_ε is finally

$$\ell_\varepsilon/\delta_e = \kappa(1 - r'^4)/4. \tag{9}$$

We emphasize that eq. (9) applies to both channel and TBL under the same planar wall condition.

Similarly, for τ, we obtain

$$\tau/\tau_w = 1 - (y/\delta_e)^\gamma = 1 - (1 - r')^\gamma, \tag{10}$$

where $\gamma = 1 + \beta$ is also an exponent to be determined. For channel, we have an exact result: $\tau = \tau_w r'$, hence eq. (10) is rigorous with $\gamma = 1$. For TBL, it has been noticed that $\gamma \neq 1$ [23]. Here, we argue that $\gamma > 1$, as it would signify a larger magnitude of the Reynolds stress (since $W \approx \tau$), hence also a larger turbulent production (SW) as observed by Jimenez et al. [24]. Inspecting DNS data [25], we propose an empirical $\gamma = 3/2$ for TBL, which keeps invariant for all Re's.

Substituting $\Theta = \varepsilon/(SW)$ into eq. (7) yields $S = \sqrt{W}/(\ell_\varepsilon\Theta^{1/4})$. Integrating S in r and using $W \approx \tau$, one has

$$U_e - U = \int_0^r S\,\mathrm{d}\hat{r} \approx \int_0^r \frac{\sqrt{\tau}}{\ell_\varepsilon\Theta^{1/4}}\mathrm{d}\hat{r}. \tag{11}$$

Substituting eqs. (8), (9) and (10) into eq. (11) yields

$$(U_e - U)/u_\tau \approx \frac{1}{\kappa}\int_0^{r'} f(\hat{r})\mathrm{d}\hat{r}, \tag{12}$$

where

$$f(\hat{r}) = \frac{4\sqrt{1-(1-\hat{r})^\gamma}\,(1+{r_\mathrm{c}}^2)^{1/4}}{[1+(r_\mathrm{c}/\hat{r})^2]^{1/4}(1-\hat{r}^4)}.$$

Denoting $G(r') = \int_0^{r'} f(\hat{r})\mathrm{d}\hat{r}$, eq. (12) yields $G = \kappa U_d/u_\tau$ where $U_d = U_e - U$. This linear relation is indeed validated with high accuracy (Figure1(a)), where $r_\mathrm{c} = 0$ and $\gamma = 3/2$ (empirical) for TBL, while $r_\mathrm{c} = 0.37$ (empirical) with $\gamma \equiv 1$ for channel. Note that $\kappa = 0.45$ (empirical) is universal in both flows, as indicated by the linear slope. Also included are $\kappa = 0.40$ and 0.38, showing notable departure away from data.

Note that eq. (12) immediately yields a prediction of the mean velocity: $U^+ = U/u_\tau = U_e^+ - G/\kappa$. Comparisons with data (with known empirical U_e^+) show impressive agreement, as seen in Figure 1. The relative errors are bounded within 1%-2%, at the same level as the data uncertainty. The current description is as simple as the LPR (for channel) and much simpler than the MCN (for TBL involving over ten free parameters), but with comparable if not better accuracy. Note also that the good description extends up to $y_b^+ = u_\tau y_b/\nu \approx 50$ (the buffer layer thickness), which corresponds to the breakdown of the quasi-balance condition near the wall, an important topic discussed in detail in ref. [19].

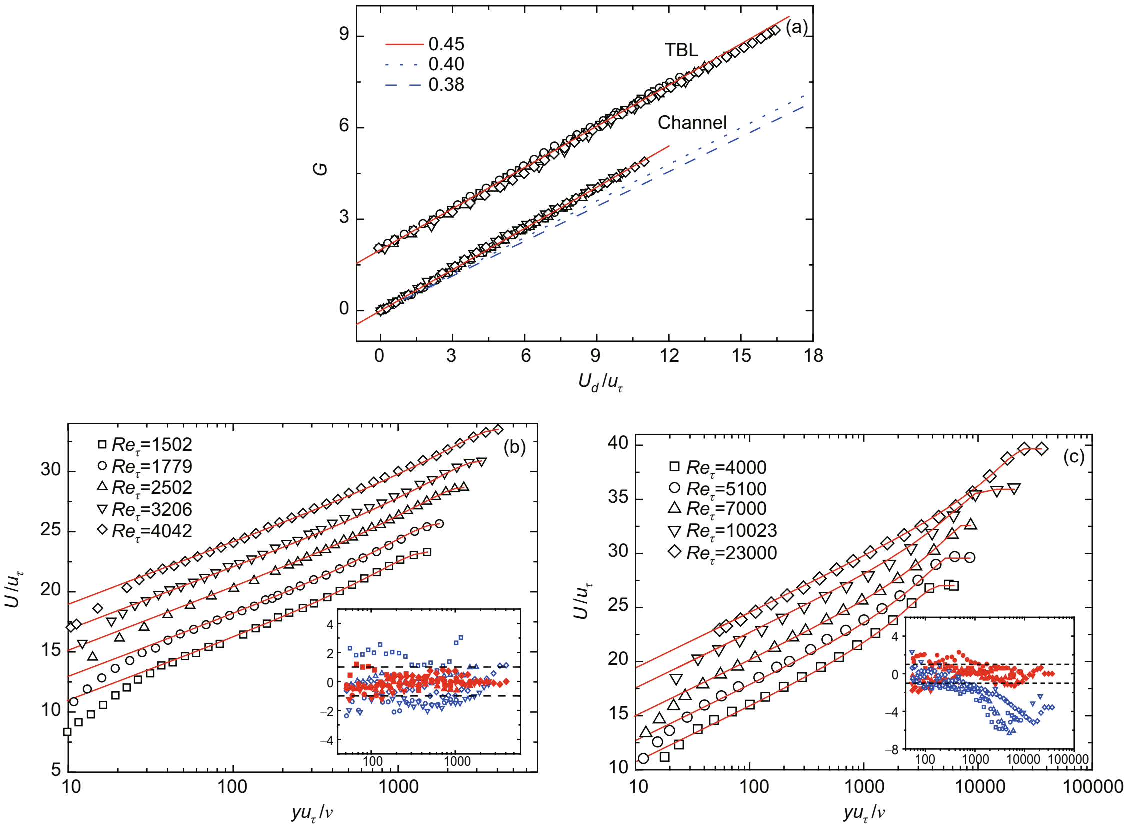

Figure 1 (Color online) (a) Validation of eq. (12) by experimental U_d/u_τ at large Re's. Solid lines indicate the universal slope $\kappa = 0.45$, dotted line $\kappa = 0.40$ and dashed line $\kappa = 0.38$; (b) predictions (lines) of MVP for channel. Inset shows the relative errors $100 \times (U^{\mathrm{Exp}}/U^{\mathrm{Theory}} - 1)$, where red solids are current predictions bounded within 1% (dashed lines), and blue opens are the LPR model [17]; (c) predictions (lines) of MVP for TBL. Red solids in the inset are current predictions within 2% (dashed lines), and blue opens are the MCN model [16]. Profiles are vertically staggered for clarity. Channel: all data from ref. [26]; TBL: $Re_\tau = 4000, 5100, 7000$ from ref. [27]; 10023 from ref. [23]; 23000 from ref. [28].

3 Predictions for turbulent boundary layer

The theory can predict streamwise development for relevant integral quantities in TBL. Three mean quantities are estimated as a preparation: U_e, $\overline{U} = \int_0^1 U\mathrm{d}r$ (vertically averaged mean velocity) and $\overline{U^2} = \int_0^1 U^2\mathrm{d}r$ (second moment of U), which yields (see the Appendix)

$$\begin{aligned} &U_e^+ \approx \kappa^{-1}\ln Re_\tau + B_e \approx \ln \mathrm{Re}_\tau/0.45 + 9.04, \\ &\overline{U}^+ \approx U_e^+ - c_1 \approx \ln \mathrm{Re}_\tau/0.45 + 5.77, \\ &\overline{U^2}^+/U_e^+ \approx \overline{U}^+ - c_1 \approx \ln \mathrm{Re}_\tau/0.45 + 2.50, \end{aligned} \tag{13}$$

here, superscript + indicates normalization with u_τ, and $B_e \approx 9.04$ is a constant involving wall function calculation and $c_1 = \kappa^{-1}\int_0^1 G(r')\mathrm{d}r' \approx 3.27$ is theoretically determined (see the Appendix). Comparison of eq. (13) with data are illustrated in Figure 2(a) showing good agreement. Note that eq. (13) implies that the familiar shape factor $H \equiv 1$, since the displacement thickness is defined by $\delta^* \equiv \int_0^{\delta_e}(1 - U/U_e)\mathrm{d}y$, thus $H \equiv \delta^*/\theta = (U_e^+ - \overline{U}^+)/(\overline{U}^+ - \overline{U^2}^+/U_e^+) = c_1/c_1 \equiv 1$. The higher order correction to eq. (13) and H is discussed in the Appendix.

A new prediction is the ratio between the momentum thickness Re ($Re_\theta = \theta U_e/\nu$) and the friction velocity Re ($Re_\tau = \delta_e u_\tau/\nu$) at the same x (distance to the leading edge of a TBL). Substituting eq. (13) into eq. (14), we obtain

$$\alpha \equiv Re_\theta/Re_\tau = \overline{U}^+ - \overline{U^2}^+/U_e^+ \approx c_1 \approx 3.27, \tag{14}$$

as shown in Figure 2(b). We can then connect Re_θ (and Re_τ) with the streamwise Re ($Re_x = U_e x/\nu$), using eq. (14). Note that eq. (4) indicates $\mathrm{d}Re_x/\mathrm{d}Re_\theta = \mathrm{d}x/\mathrm{d}\theta = U_e^{+2}$, which, by noting $U_e^+ \approx \kappa^{-1}\ln(Re_\theta/\alpha) + B_e$ and integrating in Re_θ (or U_e^+) (dropping a higher order term in $1/\ln(Re_\theta)$), leads to

$$\begin{aligned} Re_x/Re_\theta &\approx (U_e^+ - 1/\kappa)^2 + \kappa^{-2} \\ &\approx \kappa^{-2}[(\ln(Re_\theta/\alpha) + \kappa B_e - 1)^2 + 1] \\ &\approx 4.94[(\ln Re_\theta + 1.88)^2 + 1]. \end{aligned} \tag{15}$$

Compared to the MCN formula [16]: $Re_x/Re_\theta = 6.7817\ln^2 Re_\theta + 3.6241\ln Re_\theta + 44.2971 + 50.5521/\ln Re_\theta + \ldots$, eq. (15) is much simpler (Figure 2(c)), and the coefficients are completely determined by three parameters (κ, α and B_e).

Perhaps the most interesting prediction is the streamwise development of u_τ. According to eq. (13), $\ln Re_\tau = \kappa U_e/u_\tau - \kappa B_e$. Since $Re_\theta = \alpha Re_\tau = \alpha\exp(\kappa U_e/u_\tau - \kappa B_e)$, eq. (15) thus further yields a useful relation

$$Re_x \approx (\alpha/\kappa^2)\exp(\kappa U_e/u_\tau - \kappa B_e)[(\kappa U_e/u_\tau - 1)^2 + 1]. \tag{16}$$

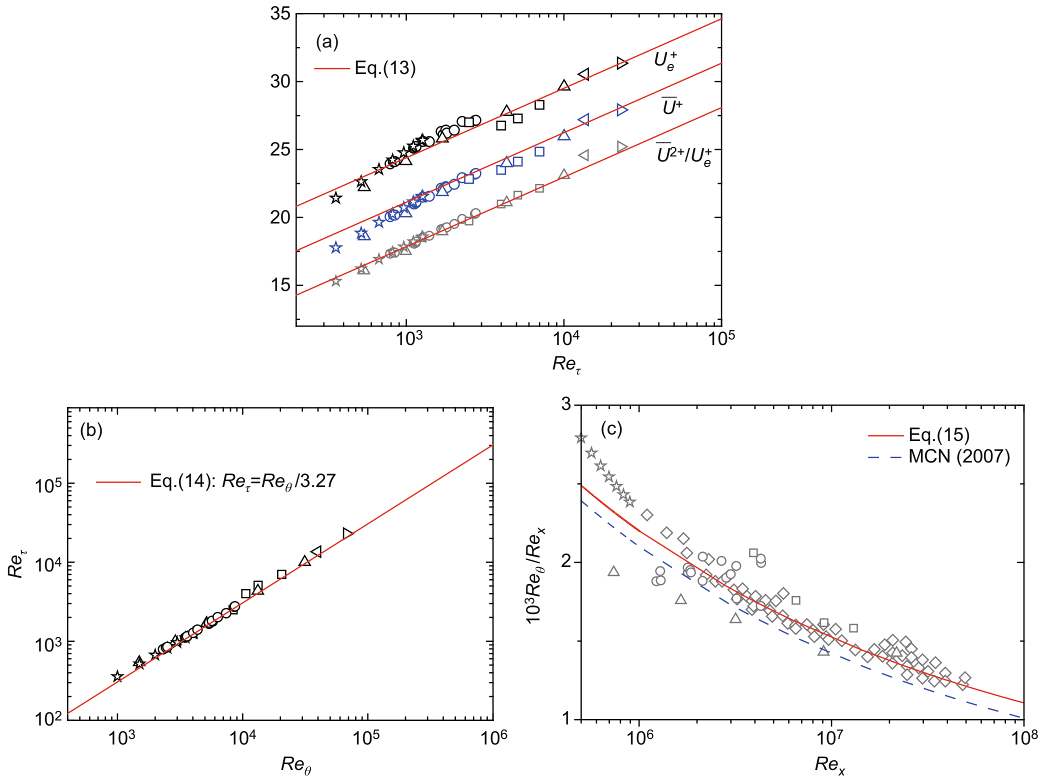

Figure 2 (Color online) (a) Data of U_e^+ (black), $\overline{U}^+$ (blue) and $\overline{U^2}^+/U_e^+$ (gray) as functions of Re_τ, compared with eq. (13) (lines) showing good agreement; (b) Re_τ as a function of Re_θ predicted by eq. (14); (c) the ratio of $10^3 Re_\theta/Re_x$ as a function of Re_x. In all panels, ★ are DNS data from ref. [25]; all others are EXP data, i.e. △ from ref. [23], □ from ref. [27], ▷ from ref. [28], ○ from ref. [29], ◁ from ref. [30], ◇ from Figure 8 of ref. [16].

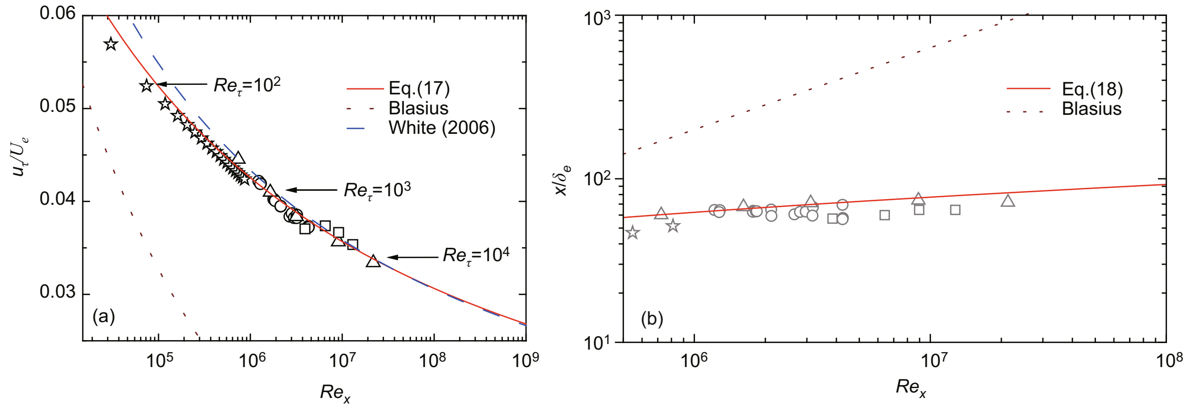

Figure 3 (Color online) (a) Friction velocity as a function of Re_x compared to the predictions in eq. (17) (arrows depict the order of Re_τ); (b) the ratio of x/δ_e as a function of Re_x. Data are the same as in Figure 2.

Taking the logarithm of eq. (16), one has

$$\begin{aligned} U_e/u_\tau &\approx \kappa^{-1}\ln Re_x + B_e - \kappa^{-1}\ln(\alpha/\kappa^2) + O(\ln(\ln Re_x)) \\ &\approx \ln Re_x/0.45 + 2.86 - 3.83\ln(\ln Re_x), \end{aligned} \tag{17}$$

where the coefficient (−3.83) for $\ln(\ln Re_x)$ term is obtained by an exact solution of eq. (16): $U_e/u_\tau \approx 42$ at $Re_x = 10^{10}$. Figure 3(a) shows eq. (17) compared with data; the agreement is very satisfactory, notably better than the White's [31] fitting formula $U_e/u_\tau = \ln(0.06Re_x)/0.477$ at moderate Re_x.

The streamwise growth of the boundary layer thickness is derived similarly. From eq. (14), $\delta_e/\theta = U_e^+/\alpha \approx 0.68\ln Re_\tau + 2.76$. Furthermore, using eqs. (15) and (17), we obtain

$$\begin{aligned} x/\delta_e &= \alpha Re_x/(U_e^+ Re_\theta) \approx \alpha[U_e^+ - 2/\kappa + 2/(\kappa^2 U_e^+)] \\ &\approx 7.27\ln Re_x - 5.18 - 12.52\ln(\ln Re_x), \end{aligned} \tag{18}$$

by neglecting the highest order term $(2/(\kappa^2 U_e^+))$. This full analytic prediction is made for the first time, after Blasius's similar result ($x/\delta_e \approx 0.2Re_x^{1/2}$) for a laminar boundary layer. The agreement between data and eq. (18) is generally good, within uncertainty in the definition of the leading edge of a TBL due to the tripping force which introduces different virtual origins (shifting the location of $x = 0$) among different data sets in the calculation of Re_x. However, this uncertainty (due to the tripping force) becomes small at high Re, and thus, the present comparison is still meaningful. Note that we have, for the first time, made a concise prediction of the streamwise development of the turbulent boundary layer thickness, in parallel to Blasius's $\sqrt{Re_x}$ prediction of the laminar boundary layer over a century ago.

Finally, the scaling of the vertical velocity at the boundary layer edge (V_e) can also be predicted. Since $V_e = -\int_0^{\delta_e} \partial_x U \mathrm{d}y = U_e(\mathrm{d}\delta^*/\mathrm{d}x)$ from eq. (2), and $\delta^* = \delta_e(1 - \overline{U}^+/U_e^+) = c_1\delta_e/U_e^+$ from eq. (13), one has (using eqs. (17) and (18))

$$V_e/U_e = \mathrm{d}\delta^*/\mathrm{d}x \propto 1/\ln^2 Re_x, \tag{19}$$

in contrast to $V_e/U_e \propto Re_x^{-1/2}$ in a laminar boundary layer.

4 Summary

In summary, a complete analytic theory for streamwise development of mean quantities ($u_\tau, \delta_e, \theta \ldots$) in TBL is presented, validated by reliable data. The unified description of channel and TBL relies on the crucial assumption about the dilation center $r = 0$ located at the centerline of the channel and the edge of the boundary layer, which derives the same defect law for the length ℓ_ε. In this description, only three parameters are introduced, in which $\kappa = 0.45$ and $m = 4$ are universal, while a core layer thickness $r_c = 0.37$ for channel and a fractional exponent $\gamma = 3/2$ for TBL, respectively. To recover the streamwise scaling, an additional fitting parameter $B_e = 9.04$ is introduced. They are still few compared to the most recent theoretical models such as refs. [15, 16]. The most important of all is that our symmetry-inspired formula applies to circular pipes, rough walls, compressible TBLs, Rayleigh-Bernard convection, etc., to be communicated soon.

This work was supported by the National Natural Science Foundation of China (Grant Nos. 11452002 and 11521091). We thank gratefully for many discussions with F. Hussain.

1 P. A. Davidson, Y. Kaneda, K. Moffatt, and K. R. Sreenivasan, *A Voyage Through Turbulence* (Cambridge University, Cambridge, 2011).

2 A. J. Smits, and I. Marusci, Phys. Today **66**, 25 (2013).

3 L. J. Yue, H. B. Lu, X. Xu, and X. Y. Chang, Sci. China-Phys. Mech. Astron. **58**, 104703 (2015).

4 X. Zhang, C. Pan, J. Q. Shen, and J. J. Wang, Sci. China-Phys. Mech. Astron. **58**, 064702 (2015).

5 Y. B. Chu, L. Wang, and X. Y. Lu, Sci. China-Phys. Mech. Astron. **57**, 2316 (2014).

6 J. Q. Shen, C. Pan, and J. J. Wang, Sci. China-Phys. Mech. Astron. **57**, 1352 (2014).

7 Z. W. He, X. L. Li, and X. Liang, Sci. China-Phys. Mech. Astron. **57**, 753 (2014).

8 L. Prandtl, In *Third International Mathematical Congress* (Heidelberg, 1904), pp. 484-491; L. Prandtl, Z. Angew. Math. Mech. **5**, 136 (1925).

9 O. Reynolds, Phil. Trans. R. Soc. London Ser. A **174**, 935 (1883).

10 I. Marusic, B. J. McKeon, P. A. Monkewitz, H. M. Nagib, A. J. Smits, and K. R. Sreenivasan, Phys. Fluids **22**, 065103 (2010).

11 V. Yakhot, Phys. Rev. E **82**, 045301(R) (2010).

12 C. B. Millikan, In *Proceedings of 5th International Congress on Applied Mechanics* (Cambridge, 1938), pp. 386-392.

13 G. I. Barenblatt, and A. J. Chorin, Proc. Natl. Acad. Sci. USA **101**, 15023 (2004).

14 W. K. George, AIAA J. **44**, 2435 (2006).

15 T. B. Nickels, J. Fluid Mech. **521**, 217 (2004).

16 P. A. Monkewitz, K. A. Chauhan, and H. M. Nagib, Phys. Fluids **19**, 115101 (2007).

17 V. S. L'vov, L. Procaccia, and O. Rudenko, Phys. Rev. Lett. **100**, 054504 (2008).

18 Z. S. She, Y. Wu, X. Chen, and F. Hussain, New J. Phys. **14**, 093054 (2012).

19 Z. S. She, X. Chen, and F. Hussain, arXiv: 1112.6312.

20 X. Chen, F. Hussain, and Z. S. She, arXiv: 1606.00212.

21 A. E. Perry, and M. S. Chong, J. Fluid Mech. **119**, 173 (1982).

22 J. Jimenez, Annu. Rev. Fluid Mech. **44**, 27 (2012).

23 D. B. Degraaff, and J. K. Eaton, J. Fluid Mech. **422**, 319 (2000).

24 J. Jimenez, S. Hoyas, M. P. Simens, and Y. Mizuno, J. Fluid Mech. **657**, 335 (2010).

25 P. Schlatter, Q. Li, G. Brethouwer, A. V. Johansson, and D. S. Henningson, Int. J. Heat Fluid Flow **31**, 251 (2010).

26 J. P. Monty, *Developments in Smooth Wall Turbulent Duct Flows*, Dissertation for the Doctoral Degree (University of Melbourne, Melbourne, 2005).

27 J. Carlier, and M. Stanislas, J. Fluid Mech. **535**, 143 (2005).

28 T. B. Nickels, I. Marusic, S. Hafez, N. Hutchins, and M. S. Chong, Philos. Trans. R. Soc. A **365**, 807 (2007).

29 R. Orlu, *Experimental Studies in Jet Flows and Zero Pressure-Gradient Turbulent Boundary Layers*, Dissertation for the Doctoral Degree (Kungliga Tekniska Högskolan, Stockholm, 2009).

30 N. Hutchins, T. B. Nichels, I. Marusic, and M. S. Chong, J. Fluid Mech. **635**, 103 (2009).

31 F. M. White, *Viscous Fluid Flow* (McGraw-Hill, New York, 2006).

Appendix

Note that $U_e^+ - \overline{U}^+ = \int_0^1 U_d^+ \mathrm{d}r'$. Assuming eq. (12) extends to the wall, the near-wall contribution up to the buffer layer is estimated to be $O(\ln Re_\tau/Re_\tau)$ and is neglected; we thus have $\int_0^1 U_d^+ \mathrm{d}r' \approx c_1$ where $c_1 = \kappa^{-1}\int_0^1 G(r')\mathrm{d}r'$, with $G(r') = \int_0^{r'} f(\hat{r})\mathrm{d}\hat{r}$ in eq. (12). We further rewrite $G(r') = \int_0^{r'}(1-\hat{r})^{-1}\mathrm{d}\hat{r} + \int_0^{r'} g(\hat{r})\mathrm{d}\hat{r}$, where $g(\hat{r}) = f(\hat{r}) - (1-\hat{r})^{-1}$ is a smooth function bounded in the domain $0 \leqslant \hat{r} \leqslant 1$, to remove a singularity $f(\hat{r}) \propto (1-\hat{r})^{-1}$ at $\hat{r} = 1$ and to obtain a finite g. Since $\int_0^1\int_0^{r'}(1-\hat{r})^{-1}\mathrm{d}\hat{r}dr' = 1$, $\int_0^1\int_0^{r'} g(\hat{r})\mathrm{d}\hat{r}\mathrm{d}r' \approx 0.47$ (numerical integration), we thus have $c_1 = \kappa^{-1}(1+0.47) \approx 3.27$. Similarly, $\int_0^1 U_d^{+2}\mathrm{d}r = U_e^{+2} + \overline{U^2}^+ - 2U_e^+\overline{U}^+ \approx c_2$ where $c_2 = \kappa^{-2}\int_0^1 G^2(r')\mathrm{d}r' \approx 19.55$. It leads to $\overline{U^2}^+/U_e^+ \approx 2\overline{U}^+ - U_e^+ + c_2/U_e^+ \approx \overline{U}^+ - c_1 + c_2/U_e^+$, and $H = c_1/(c_1 - c_2/U_e^+) > 1$ for finite Re ($H \approx 1.26$ at $Re_\tau = 10^4$). Finally, let us calculate B_e. As eq. (12) extends to y_b^+ (buffer layer thickness), then $U_e^+ = U_b^+ + \kappa^{-1}\int_0^{1-y_b^+/Re_\tau} f(\hat{r})\mathrm{d}\hat{r}$, which yields $U_e^+ = \ln Re_\tau/\kappa + B_e$, where $B_e = (U_b^+ - \kappa^{-1}\ln y_b^+) + \kappa^{-1}\int_0^{1-y_b^+/Re_\tau} g(\hat{r})\mathrm{d}\hat{r}$, determined by y_b^+ and U_b^+ (its precise values will be discussed elsewhere). Here, we let $B_e = 9.04$ to fit all data in Figure 2, which is the only fitting parameter to yield eq. (13).